

**GMAO RESEARCH BRIEF**

December 2019

El Niño Related Tropical Land Surface Water and Energy Response in MERRA-2

Michael G. Bosilovich, NASA GSFC GMAO; Franklin R. Robertson, NASA MSFC and Paul W. Stackhouse, NASA LaRC; *Presented at the 2019 AGU Fall Meeting, Dec 9, 2019 (A11U-2846)*

SUMMARY

Tropical land warming response to El Niño is a well-known and well-observed occurrence. The fundamental processes by which the warming occurs is, however, not well understood. In this study, we combine several El Niño events as represented by MERRA-2, to develop a composite El Niño in order to isolate the most consistent processes. Results show that the El Niño sea surface temperature (SST) warming eventually causes less clouds over land and more solar energy to reach and warm the surface. While precipitation is also reduced, it takes additional time for the soil water to dry and realize the full effect on the land temperatures. The GEOS model used in MERRA-2 also demonstrates these same features, though, most significant closer to the El Niño SST warming.

BACKGROUND

The MERRA-2 reanalysis assimilates many observations from NASA and the operational system. It provides a high-quality depiction of the weather throughout a nearly 40-year period and includes output diagnostics that are not routinely observed. Here, we use it to understand the water and energy cycle variations occurring during El Niño events. In addition, we evaluate the GEOS atmospheric model response to the anomalous forcing and to better understand the influence of satellite observations on the analyzed weather during El Niño.

Introduction

The El Niño Southern Oscillation (ENSO) is a coupled Earth system circulation phenomena that reaches all around the globe. The heat added to the atmosphere by increased precipitation produces circulation changes that have global reach and, over time, warms the entire tropical band, and much of the Earth. Many studies have noted that El Niño causes warm and dry (and sometimes drought) conditions over tropical land masses. We develop a composite analysis of El Niño to identify the predominate features of tropical land response. This analysis shows that the land's lagged response is related to a reduction clouds that leads to increase surface shortwave (SW) radiation that increases the surface temperature. The precipitation lag is somewhat longer, and then leads to a reduction in soil water and, in concert with increased SW induced surface warming, leads to increased sensible heating of the atmosphere above. The MERRA-2 Atmospheric Model Intercomparison Project (M2AMIP) simulation generally captures these features, but the response is strongest with increased temporal and spatial proximity to the El Niño peak warming. The regionality of these features is also discussed, and it is noted that even the strongest individual El Niño events can vary from this composite mechanistic paradigm.

Observational Evaluation

Visually, the response of the tropical land to ENSO is generally apparent in the time series of reanalyses (Figure 1). The shaded Niño3.4 SST anomalies, compared with tropical land meteorology, show the lagged response, as well as some event by event discrepancies. During el Niño events, precipitation is reduced with reduced clouds and increased solar radiation (related to a reduction in clouds). The land temperatures are generally warmer after El Niño, lagged by ~3-4 months. While this has been noted in literature, and generally apparent in models, reanalyses and observations (Figure 1), the processes by which the land is forced has not been broadly defined.

Composite Analysis

Here, we composite eight El Niño events to determine the common features among them. Figure 2 shows the result of the composite technique for several key quantities in MERRA-2. The composite analysis shows that significant temperature increases only occur sometime after precipitation reductions (Figure 2a) and increased solar forcing, less clouds (Figure 2b). The temperature follows the increase on surface sensible heating (Figure 2c), and reductions in surface evaporation and soil wetness (Figure 2e).

The surface temperature warming is not significantly related to net longwave heating of the surface (Figure 2d) or the atmospheric convergence of energy over the tropical lands (Figure 2f). The model-only simulation of the present-day climate (M2AMIP) shows many of these same features, but the relationships degrade farther away, in space and time, from the core of the El Niño SST forcing (expanded on in the accepted paper, Bosilovich et al., 2019).

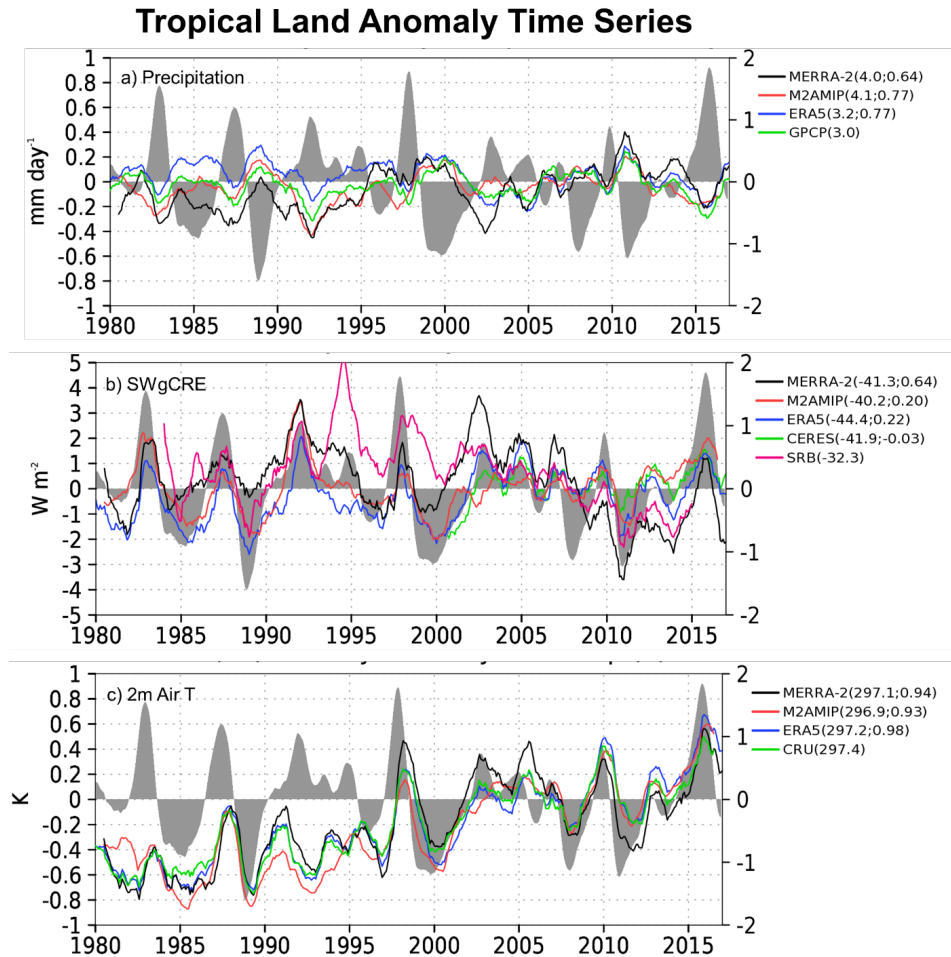


Figure 1: Comparison of anomalies of tropical (a) precipitation, (b) surface shortwave cloud radiative effect (SWCRE), and (c) near surface air temperature over land (30S-30N) regions for MERRA-2, M2AMIP, and ERA5 data with observations from CERES/SRB, GPCP and CRU, respectively. The anomalies remove the common mean annual cycle period (2000-2014) and have a 12-month running mean applied. The time averaged mean of the data is reported in the legend. Niño 3.4 SST anomalies (K) are grey shaded with the scale on the right axis (anomalies are 12-month running means). Mean values and correlations coefficients to the reference observations are shown in the legend.

The composite analysis in Figure 2 show low frequency connections through monthly means. In order to better understand the faster modes of variability and relationships among the processes, we also look at the El Niños in a pentad (5-day) frequency composite analysis. Figure 3 shows the lead/lag correlations for several quantities as related to the land surface temperature and precipitation/evaporation.

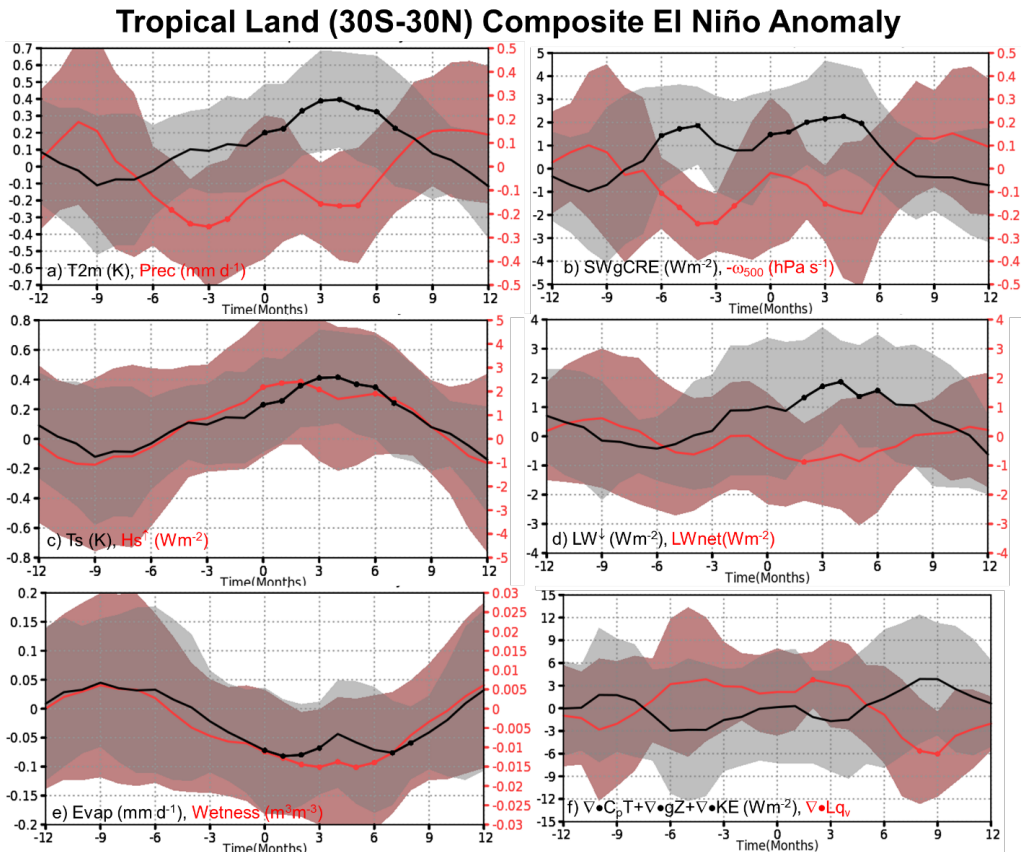


Figure 2: Tropical global monsoon land areas (30S-30N) composite El Niño anomaly time series for MERRA-2 (left) and M2AMIP (right) for several key quantities listed on the figure. The solid line indicates the composite average and shading indicates ± 1 standard deviation of the composite mean. Scales are color coded for each line. Dots indicate anomalies significantly different from zero (at 90% confidence). The variables are near surface air temperature (T2m), precipitation, SWgCRE, vertical velocity ($-\omega_{500}$, directed positive for upward motion, at the 500hPa level), surface temperature (Ts), sensible heat flux (Hs), downward longwave radiation (LW^d) and net surface longwave radiation (LWnet, directed downward positive), dry static energy (DSE) divergence ($\nabla \cdot C_p T + \nabla \cdot gZ + \nabla \cdot KE$), heating due to water vapor divergence ($\nabla \cdot Lq_v$), surface evaporation (Evap) and surface soil wetness. DSE and water vapor divergence are computed from the model output fluxes of q_v , $C_p T$ and gZ , and do not include mass corrections to the wind.

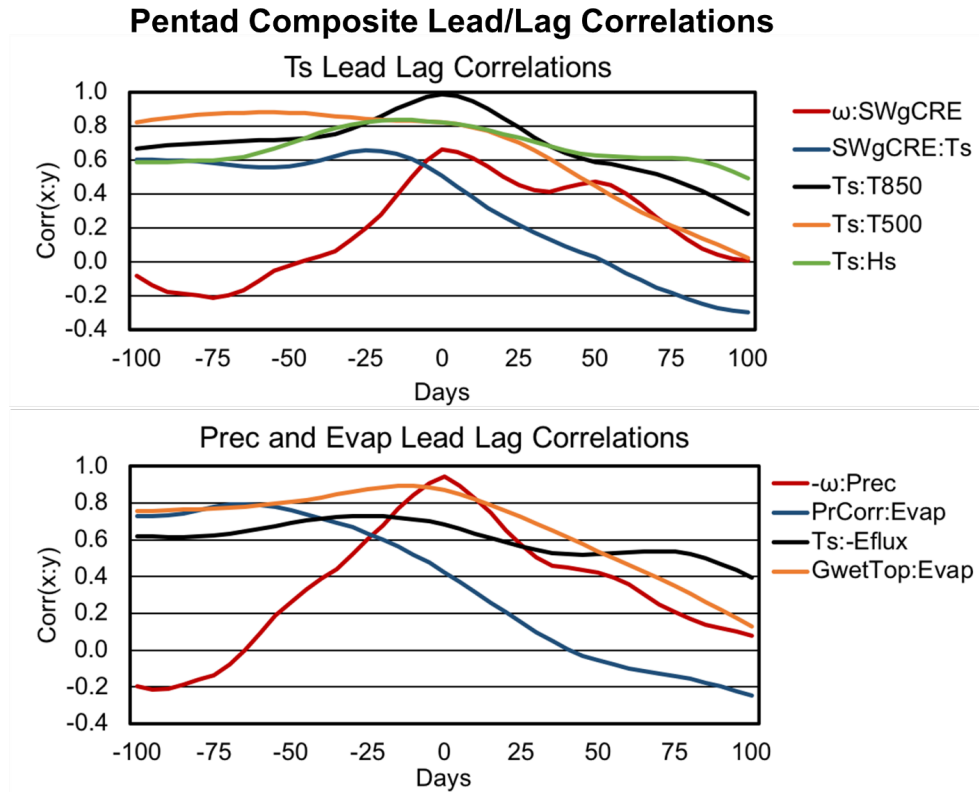


Figure 3: Tropical land global monsoon region lead lag correlations for a) surface temperature variables and b) water cycle variables. The correlations are developed by from the MERRA-2 pentad time series, with leading correlations as negative days and lag correlations are positive days for pairs of variables $x:y$, where the first variable (x) is computed as leading or lagging the second variable (y). Correlation units are dimensionless, and the values are computed over 101 data points (8 months of pentads) and values of 0.26 are significant at 99% confidence. Here, 0 days refers to contemporaneous correlation of pentads, not the $M=0$ El Niño peak.

Physical Processes

The time correlations are computed for 101 pentads (+8 months) relative to the pentad with peak El Niño 3.4 SST. Lead/lag correlations are determined by shifting the first variable listed, relative to the second. In this way, we highlight the modes of variation between the relevant quantities during the evolution of El Niño. For example, 500 hPa vertical velocity and SWgCRE correlate most strongly at zero lag, indicating a mode of rapid response of one to the other. Given the large-scale change over the composite El Niño, this represents the cloud responding to the dynamical variations represented in vertical velocity.

On the other hand, SWgCRE leads surface temperature (T_s), even out to leads of 100 days (~3 months), suggesting the effects of persistent radiative forcing. However, there is a maximum correlation at a lead of 25 days. The surface temperature leads sensible heating, but with a broad peak correlation with an approximate lead of 10-15 days. This contributes to a rapid response of T850 to the surface temperature, which correlate to 0.99 at lag zero indicating strong mixing within the planetary boundary layer. These results show the importance of multiple temporal scales (weather to interannual) governing the nature of the surface warming as the circulation reduces clouds over land, increases the shortwave and warms the surface and the lower troposphere.

The water cycle is strongly coupled to these processes. In Figure 3b, as could be expected, precipitation (model-generated) is highly correlated with vertical motion at zero lag. Precipitation that forces soil moisture (note for MERRA-2 this is the observation-corrected precipitation) leads evaporation, primarily at longer lead times. This reflects the influence of the soil water storage on the evaporation and the time it takes to deplete the soil water and warm the surface, as the soil wetness also has a peak correlation leading the evaporation (by 15 days). Surface temperature is already increasing by the time evaporation is decreasing, indicating the effect on cloud and shortwave radiation leads the surface temperature increase before the precipitation soil moisture effects, though at 3-4 months after the peak of El Niño, both mechanisms are playing a role in the tropical continental warming and drying.

This study has been accepted for publication at the AMS Journal of Climate
Bosilovich, M.G., F.R. Robertson, and P.W. Stackhouse: El Niño Related Tropical Land
Surface Water and Energy Response in MERRA-2. J. Climate,
<https://doi.org/10.1175/JCLI-D-19-0231.1>